Eksploatacja i Niezawodnosc – Maintenance and Reliability
Volume 23 (2021), Issue 1
journal homepage: http://www.ein.org.pl

Article citation info:
Kępczak N, Bechciński G, Rosik R. Experimental verification of the deep hole boring bar model. Eksploatacja i Niezawodnosc – Maintenance and Reliability 2021; 23 (1): 55–62, http://dx.doi.org/10.17531/ein.2021.1.6.

Indexed by:
Web of Science Group

Experimental verification of the deep hole boring bar model

Norbert Kępczak [a]*, Grzegorz Bechciński [a], Radosław Rosik [a]

[a] Institute of Machine Tools and Production Engineering, Faculty of Mechanical Engineering, Lodz University of Technology, ul. Stefanowskiego 1/15, 90-924 Lodz, Poland

Highlights

- In the article theoretical and experimental tests of deep hole boring bar were performed.
- During tests of the dynamic properties divergency in the results values was below 8%.
- During tests of the static properties divergency in the results values was below 3%.
- High convergence of the results of numerical and experimental research was obtained.

Abstract

The article presents the results of the experimental verification of the deep hole boring bar tool model. The aim of the work was to obtain a verified boring bar tool model, which in further scientific research will be a starting point for creating a prototype of a tool with a new design, in which dynamic properties will be improved. The research was divided into two stages. In the first stage, modal studies of the model and the real object were carried out. The obtained discrepancy between numerical and experimental results below 8% allows to state that the model is characterized by dynamic properties occurring in the real boring bar. In the second stage of the research, static tests were carried out. The object was loaded with forces of 98.6 N, 195.0 N, 293.8 N. The obtained slight discrepancy in the results of numerical and experimental tests below 3% allows to state that the model reflects the static properties of the real boring bar. The high convergence of the theoretical and experimental results allows for the conclusion that the numerical model has been verified positively.

Keywords

boring bar, modal analysis, FEM, dynamic properties, static properties

1. Introduction

Various types of vibrations occur during the machining process. Vibrations that occur between the workpiece and the tool, even during undisturbed machining operations, are very important. Vibrations have a negative effect on the quality of the treated surface and can damage the machining center or the tool. Vibrations occurring during the cutting of the processed material can be divided into forced and self-excited [25, 32]. Forced vibrations arise as a result of a periodically acting excitation force. Self-excited vibrations, in contrast to forced vibrations, are not caused by external disturbances, but by the dynamic interaction between the mechanical system and the machining process [3, 20, 29].

Many studies have developed various approaches to reduce the occurrence of vibration in the cutting process. Active prevention of vibrations (damping) in the turning process is one of the possibilities of improving the stability of the machining process. One of the examples is the use of a mainly sinusoidal or triangular spindle speed change signal [2]. Another research approach is focused on the selection of parameters related to machining, such as feed, cutting speed or depth of cut [19]. In addition, directly process-oriented approaches include solutions with an additional damping system that is installed on the machine tool. The distinguishing feature of such a system is the need to connect an external energy source and adapt it to the existing conditions of the machine tool.

The increase in damping by passive auxiliary systems is based on the conversion of the oscillation energy into another type of energy, e.g. thermal energy. For this purpose, special tools with multi-part friction dampers integrated in the central bore of the tool are developed [11, 14, 26, 29]. Moreover, there are solutions in which the damping is realized by an additional freely swinging mass [28]. Another known passive auxiliary system is an auxiliary damper that uses the damping properties of the material (polymers, elastomers). This solution is used, for example, in boring bars [29] and turning tools [31].

The auxiliary system measures the system vibrations with sensors, processes the data with the controller, and then reduces it by introducing it into the anti-vibration system. Anti-vibrations are generated by an inductor. Active energy is always supplied to the system from outside.

A completely different approach to reducing vibration is to influence the stability of the tool and machining center by means of dynamic compliance. Equation (1) for the frequency response of the transition function is based on this approach [29]:

(*) Corresponding author.
E-mail addresses: N. Kępczak - norbert.kepczak@p.lodz.pl, G. Bechciński - grzegorz.bechcinski@p.lodz.pl, R. Rosik - radoslaw.rosik@p.lodz.pl

$$G(i\omega)=\frac{\frac{1}{c}}{1+2iD\frac{\omega}{\omega_n}-\left(\frac{\omega}{\omega_n}\right)^2} \tag{1}$$

Value $(\omega=\omega_n)$ causes occurring a resonance – equation (2).

$$\left|G(\omega=\omega_n)\right|=\frac{\frac{1}{c}}{2D}=\frac{\sqrt{\frac{m}{c}}}{d} \tag{2}$$

Than equation (3) leads to equation (4).

$$\sqrt{\frac{m}{c}}=\frac{1}{\omega_n} \tag{3}$$

$$\left|G(\omega=\omega_n)\right|=\frac{1}{d\omega_n} \tag{4}$$

where:

c – static stiffness ;
d – damping ratio;
D – degree of damping;
$G(i\omega)$ – resilience frequency response;
m – mass;
ω – forced angular frequency;
ω_n – natural angular frequency.

This approach shows that if the smaller ratio of the mass „m" to the static stiffness „c", than the higher angular frequency of the natural vibrations and if the higher damping ratio „d", than the lower value of the resilience frequency response „G", which results a lower amplitude value at resonance.

It is important to precisely determine the frequency values where the phenomenon of resonance occurs. Currently, at the design stage, numerical analyzes can be made. The designer receives the forms of natural vibrations and their frequencies [12]. However, the numerical model is always the ideal model with no disadvantages. In order to confirm the theoretical results, the so-called an identification experiment that allows for full verification of the numerical model. This article presents the comparative results of the experimental verification of the deep hole boring bar model. Getting to know the static and dynamic properties of the real boring bar is very important, because the research is preliminary in a project aimed at designing and producing a prototype of a deep hole boring bar tool with increased dynamic properties.

*Table 1. Mechanical properties of applied materials**

	Carbon steel	High-strength steel
Tensile strength [MPa]	420.00	448.00
Yield point [MPa]	350.00	275.80
Young's modulus [GPa]	200.00	200.00
Poisson's ratio [---]	0.29	0.29
Kirchhoff's modulus[MPa]	79700.00	128700.00
Density [g/cm^3]	7.85	7.85

** mechanical properties are listed according to the Autodesk Inventor 2020 Material Library*

2. Dynamic properties

2.1. Numerical analysis

Theoretical modal analysis (TMA) is defined as the matrix self problem dependent on the mass, stiffness and damping factors. TMA requires solving an own problem for the adopted structural model. It is a commonly used practice technique for examining the dynamic properties of mechanical objects. It is used not only in mechanical engineering [10, 15, 16, 33, 34] or space engineering [30], but also successfully used in building structures [24], agriculture [8] and rail transport [17]. The sets of frequencies, damping coefficients and the modes of free vibrations allow for the simulation of the behavior of the structure with any input, selection of controls, structure modification and in other situations. It is used in the design process when it is not possible to carry out research on a real object [6, 9, 18, 21].

TMA in CAD programs consists in determining the dynamic properties of the tested structure on the basis of a structural model. The modal model of a virtual structure is determined on the basis of e.g. the finite element method (FEM). Thanks to this method, a wide range of dynamic tests can be carried out on the basis of the digital prototype without the need to build an experimental stand equipped with a real research object.

TMA performed with the Autodesk Inventor simulation module enables the obtaining of the natural mode shapes and the corresponding natural frequencies. In the analytical procedure, the software developers did not take into account information on the values of the damping coefficients for individual vibration modes. The module can be used to identify the modes of natural vibrations and their frequencies, which in theoretical analysis is sufficient at the initial stage of construction assessment. The full set of modal information (modes, frequencies, damping coefficients) can be obtained on the basis of experimental modal analysis. Due to these software limitations regarding TMA, this paper compares the results obtained on the basis of theoretical and experimental analysis, including the modes of vibrations and their frequencies.

In order to conduct numerical tests, first a three-dimensional model of the test stand was created, which is presented in Figure 1. The model consists of: (1) base, (2) mounting holes, (3) boring bar head, (4) shank, (5) bracket and (6) mounting bolts. A model of the real PAFANA boring bar from the Smart Head System series was prepared for the tests. This boring bar is a modular tool, which includes a head marked K40-MWLNR/L08 and a shank marked A40-K40 300.

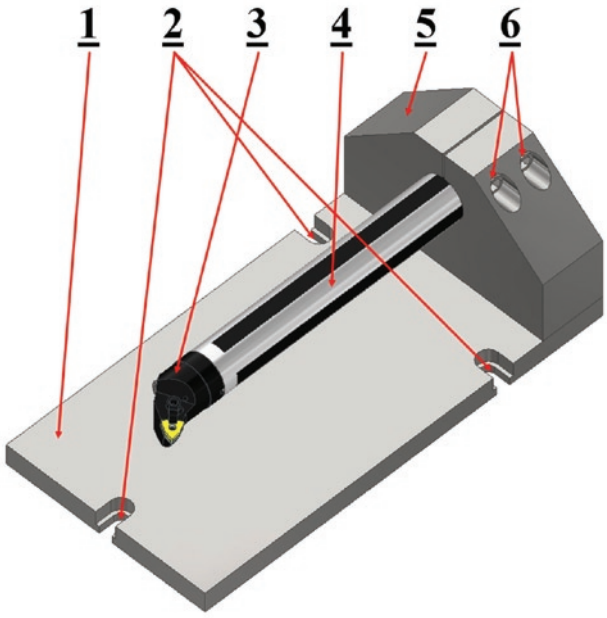

Fig. 1. Three-dimensional model of the test stand: 1 – base, 2 – mounting holes, 3 – boring bar head, 4 – shank, 5 – support, 6 – fixing screws

Next, all elements of the test stand were assigned appropriate material properties. The base and the bracket are made of carbon steel, while the boring bar is made of high-strength steel. Table 1 shows the mechanical properties for the materials used.

Then, the degrees of freedom were obtained in the places where there were mounting holes in the base (Figure 1) and a finite element mesh was implemented (Figure 2). The mesh was defined in such a way that 266329 nodes and 172856 elements were created. TMA was carried out in the frequency domain up to 3200 Hz.

Fig. 2. Finite element mesh view

2.2. Experimental research

Experimental modal analysis (EMA) is a technique that is often used in practice to investigate the dynamic properties of mechanical objects, both at the stage of designing and in operating machines. In contrast to the operational modal analysis [13], the identification experiment in the EMA consists in forcing the vibrations of the object with simultaneous measurement of the exciting force and the response of the system, most often in the form of a spectrum of vibration acceleration [6, 9, 18, 21]. One of the many applications of modal analysis is also the detection of damage to mechanical objects [35]. Apart from mechanical systems [21], experimental modal analysis is widely used in building structures [4], electronics and electrical engineering [5] and music [7].

The EMA procedure can be performed by the SISO (single input single output), SIMO (single input multiple outputs) and MIMO (multiple inputs multiple outputs) method. These methods differ not only in the requirements of measurement data acquisition systems, but also in the requirements concerning the purpose of the research and the accuracy of the analysis results. Due to hardware limitations, the SISO procedure was used in this study. Figure 3 shows the test stand with the apparatus for conducting the EMA, which includes: (1) frame, (2) modal hammer, (3) base, (4) support, (5) mounting screws, (6) accelerometer (7) boring bar, (8) data acquisition module and (9) computer with software.

For measuring and data acquisition, the PULSE Lite system from Brüel & Kjær was used, which includes:

- Piezoelectric accelerometer 4514 53958, with basic parameters [22].
- Modal hammer 8206-003 54990, with basic parameters [23].
- Data acquisition system 3560-L.

In addition, the manufacturer provides PULSE LabShop software enabling the registration and processing of collected data. The software allows to make a Fast Fourier Transform (FFT) of collected data.

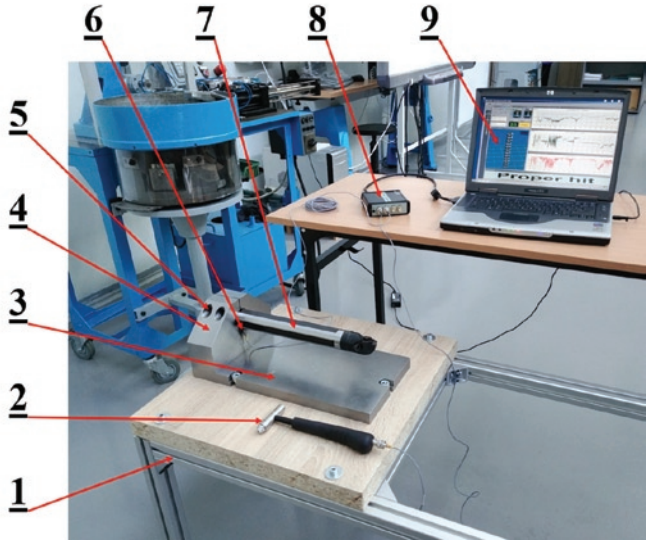

Fig. 3. The test stand: 1 – frame, 2 – modal hammer, 3 – base, 4 – support, 5 – mounting screws, 6 – accelerometer, 7 – boring bar, 8 – data acquisition module, 9 – computer

In the procedure of preparing the measurement set, a very important step is the appropriate setting of the impulse input signal level, weighting of the impulse input signal and weighting of the system response to the input excitation. The setting of the input signal level is performed by registering a certain number of repetitions of the impulse input, and then averaging the input force value. Forcing signal weighting consists in registering a specified number of excitation repetitions and passing through a "transient" window (close to rectangular) in order to register the excitation signal when the excitation reaches its maximum value. The system's response signal to a given excitation is weighting by registering a specific number of repetitions of the system's response to a given excitation and passing these signals through an exponential window, which allows the signal to be registered in its full length. The purpose of using correction windows is to minimize environmental noise and improve the quality of measurement signals.

After making the settings in the program, it was necessary to define the shape of the test object in the Pulse Lite program (Figure 4), as well as indicate the places where the excitations were performed (green and black hammers) and the place of mounting the accelerometer (red arrow). Due to the limited possibilities of spatial modeling in Pulse Lite, the shape of the boring bar was modeled approximately as a cylinder. There were 10 measuring points on the boring bar, which were excited to vibrations three times in succession. The accelerometer was placed on the boring bar as close as possible to the support. The boring bar was tested three times. The study was carried out in the frequency domain up to 3200 Hz. The sampling rate was 6400 Hz, while the time of the recording signal was 1 s.

2.3. Results and Discussion

As a result of the TMA in Autodesk Inventor, 8 modes of free vibrations were obtained in the tested frequency range. The frequency values for individual modes of free vibrations are presented in Table 2.

Only two of the generated modes of vibrations affected the boring bar directly (Mode 1 and 5). The remaining modes were associated with the vibrations of the other elements of the test stand.

As a result of the EMA, waveforms of the vibration amplitude as a function of frequency were obtained. An exemplary waveform with marked resonances is presented in Figure 5.

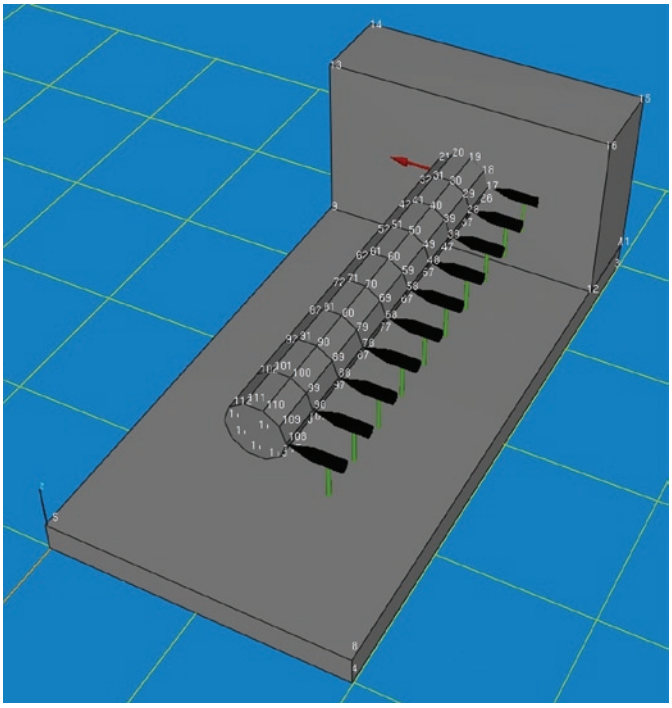

Fig. 4. The approximate geometric model of the test stand, points excited to vibrations, and the location of the displacement sensor in Pulse Lite

Table 2. Results of theoretical modal analysis

Mode	1	2	3	4	5	6	7	8
Frequency [Hz]	301	922	1685	1711	1769	2200	2473	2660

In the analyzed measuring range, the presence of three resonance peaks directly related to the vibrations of the boring bar can be clearly observed. The first resonance appeared at a frequency of 231 Hz. It was noticed that for this frequency all excited points were displaced in the same direction. This is called rigid body mode in which the entire tested object is displaced without deformation [27]. Due to the fact that the excited points were arranged in a straight line instead of in the shape of a characteristic wave, this frequency was rejected in further analysis. In the course of the amplitude of the transition function, for low frequency values, there are also smaller resonance peaks, which probably come from the vibrations of the table on which the station is mounted. In order to avoid frame vibrations, the stand should be attached, e.g. directly to the ground. In further analysis, the vibrations of the stand frame were considered insignificant and omitted.

The second resonance appeared at a frequency of 327 Hz. In this case, the excited points formed one characteristic half-wave. Figure 6 shows a comparison of the obtained forms during numerical and experimental analysis.

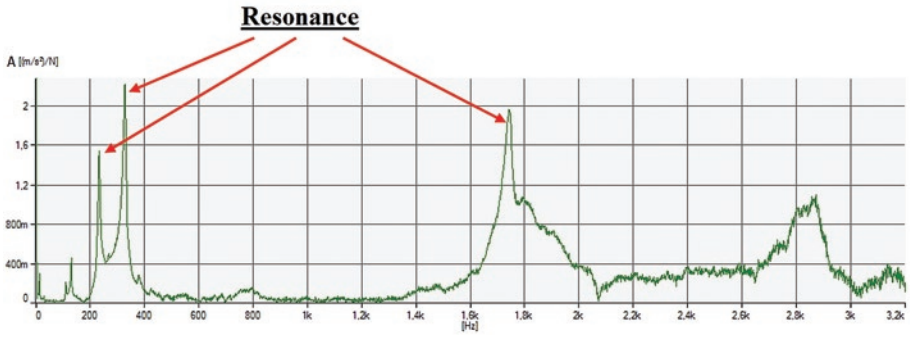

Fig. 5. An example of the amplitude waveform of the transition function

For the numerical analysis, the value of the natural frequency of the boring bar was 301 Hz, while for the experimental tests this value was 327 Hz. In the analyzed case, the divergence of the obtained results was 7.95%.

The third resonance occurred at a frequency of 1741 Hz. In this case, the excited points formed two characteristic half-waves. Figure 7 shows a comparison of the obtained forms during numerical and experimental analysis.

For numerical analysis, the value of the free vibration frequency of the boring bar was 1769 Hz, while for experimental tests this value was 1741 Hz. In the analyzed case, the divergence of the obtained results was 1.61%.

The obtained divergence of results below 8% allows to state that the model faithfully reflects the nature of the dynamic properties of the real boring bar.

3. Static properties

3.1 Numerical analysis

Static tests were carried out to determine the theoretical static strength of the boring bar. The tests were carried out for three values of the static load with the masses 10 kg, 20 kg, 30 kg. The values of the forces were estimated as sufficient to determine the static stiffness. The actual weights were prepared for the tests, which are presented in Figure 9. Then each of the weights was weighed three times with a digital dynamometer to determine the mean force of gravity. Table 3 shows the results of converting the load into the value of gravity.

In order to carry out numerical tests of the static properties of the boring bar, the tool was placed in the opposite direction to that during dynamic tests, so that the acting force of gravity acted inside the actual test stand (Figure 11). Next, all the elements of the test stand were assigned appropriate material properties in accordance with Table 1. In order to fix the boring bar in the test stand model, the degrees of freedom were removed in places where there were mounting holes in the stand base and a finite element mesh was imposed. The mesh was defined in such a way that 271271 nodes and 175984 elements were created. At the very end, appropriately calculated gravity forces were applied (Table 3). The force was applied to the cylindrical face of the boring bar head. Figure 8 shows the view of the numerical model with the finite element mesh and the loading force.

Table 3. Converting the load value to the value of gravity

Mass [kg]	10	20	30
Measurement 1 [N]	98.7	194.8	294.0
Measurement 2 [N]	98.6	195.0	293.7
Measurement 3 [N]	98.6	195.1	293.8
Average force of gravity [N]	**98.6**	**195.0**	**293.8**

3.2. Experimental research

In order to carry out experimental tests of the static properties of the boring bar on the test stand, three weights were prepared with which it was properly loaded. Figure 9 shows the view of the prepared weights.

Then the boring bar was mounted on the test stand and properly loaded. The displacement of the boring bar head was measured using two displacement sensors. One of the sensors was placed directly above the boring bar head,

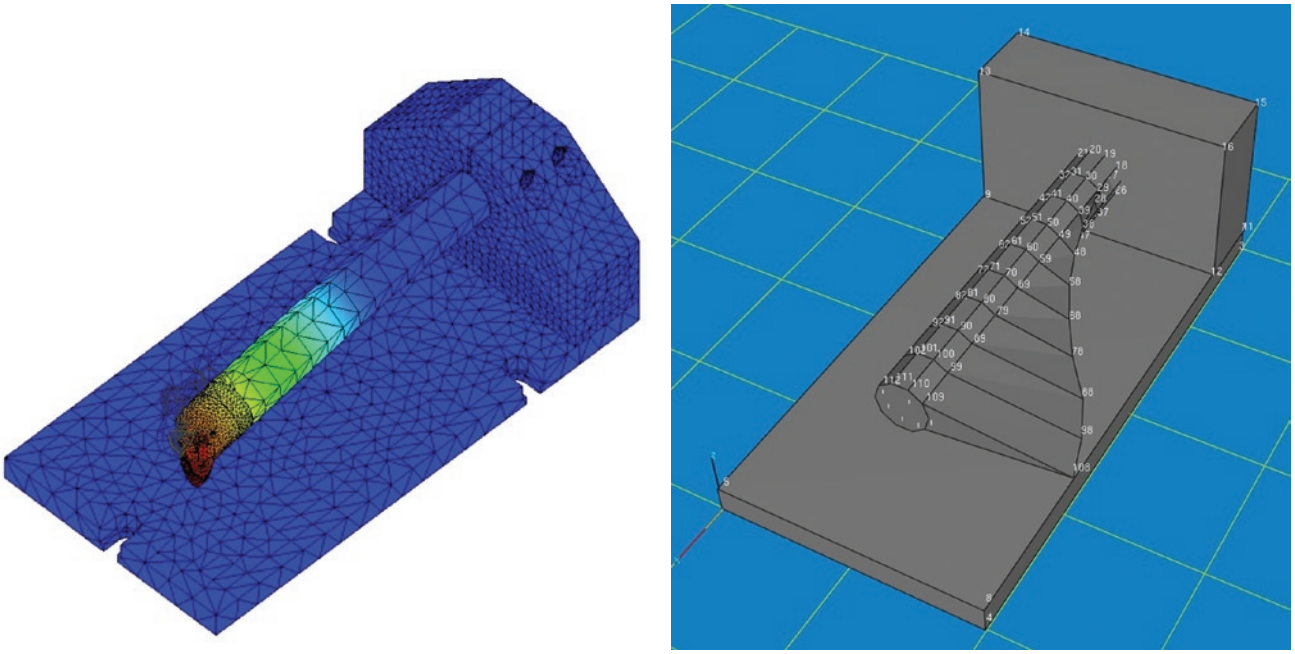

Fig. 6. Comparison of the first mode of free vibration of the boring bar obtained as a result of: a) numerical analysis for the frequency of 301 Hz, b) experimental modal analysis for the frequency of 327 Hz

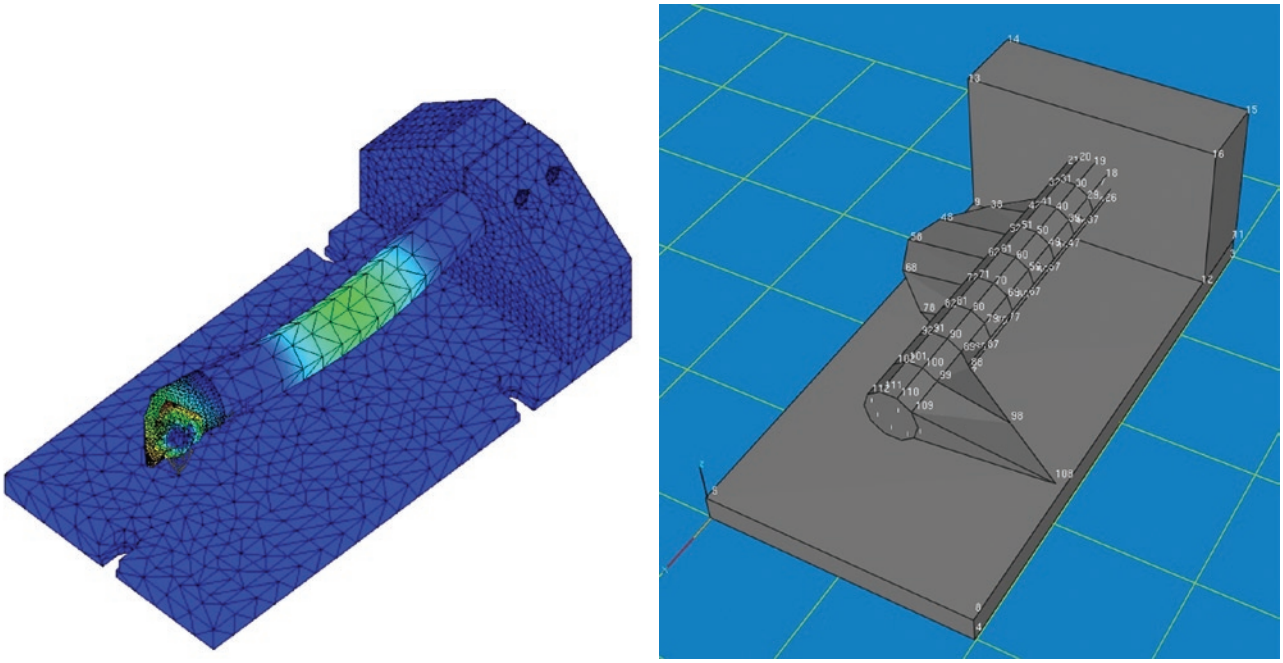

Fig. 7. Comparison of the second mode of free vibration of the boring bar obtained as a result of: a) numerical analysis for the frequency of 1769 Hz, b) experimental modal analysis for the frequency of 1741 Hz

while the other was placed under the frame of the test stand. Figure 10 shows the view of the test stand, which includes: (1) weight, (2) displacement sensor under the frame, (3) frame, (4) base, (5) support, (6) boring bar shank, (7) a boring bar head and (8) a boring bar head displacement sensor.

3.3. Results and Discussion

The experimental tests were carried out in three measurement series. The results obtained are presented in Table 4.

After subtracting the displacement indications of both sensors for individual measurements, the mean value of the displacement for the load with a force of 98.6 N was 141 μm. For a load with a force of 195.0 N, this value was 275 μm, while for a load with a force of 293.8 N, 423 μm was obtained.

Table 5 shows a comparison of the results obtained numerically with the experimental results, while Figure 11 shows the displacement of the boring bar head under the load of 293.8 N during numerical tests.

For the numerical analysis, the displacement value of the boring bar head under the load of 98.6 N was 138 μm, while for the experimental tests this value was 141 μm. In the analyzed case, the divergence of the obtained results was 2.13%. For the numerical analysis, the displacement value of the boring bar head under the load of 195.0 N was 273 μm, while for the experimental tests this value was 275 μm. In the analyzed case, the divergence of the obtained results was 0.73%. For the numerical analysis, the displacement value of the boring bar head under the load of 293.8 N was 411 μm, while for the experimental

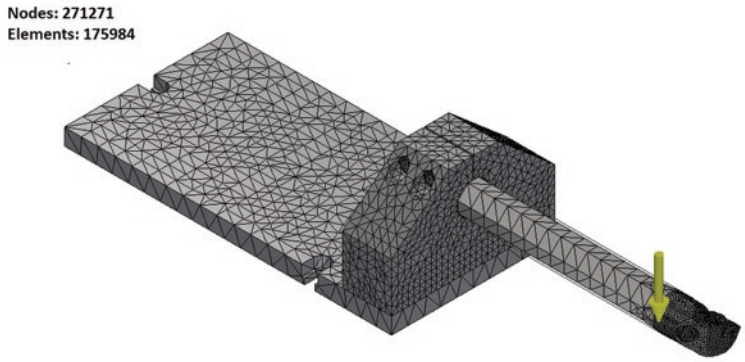

Fig. 8. View of the finite element mesh with the loading force of the test stand model with the boring bar

Fig. 9. View of the prepared weights: 1 – 10 kg, 2 – 20 kg, 3 – 30 kg

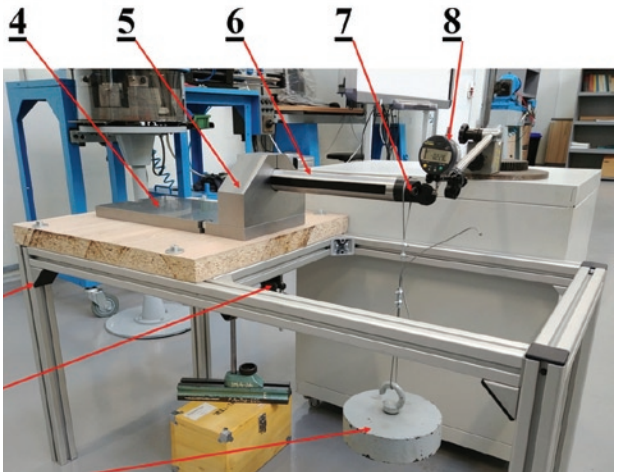

Fig. 10. View of the test stand during the loading process: 1 – weight, 2 – displacement sensor under the frame, 3 – frame, 4 – base, 5 – support, 6 - boring bar shank, 7 - boring bar head, 8 - boring bar head displacement sensor

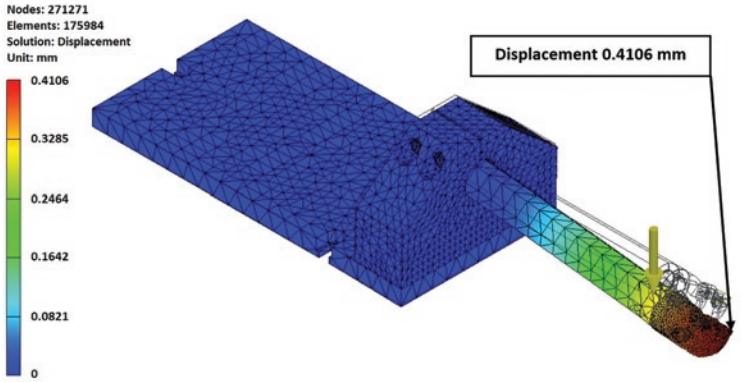

Fig. 11. The results of the numerical analysis for a force load of 293.8 N

tests this value was 423 µm. In the analyzed case, the divergence of the obtained results was 2.84%.

The obtained divergence of results below 3% allows to state that the model faithfully reflects the static properties of the real boring bar.

4. Summary and conclusions

During theoretical and experimental research, modal analyzes of deep hole boring tools were carried out. The analyzes were performed to compare the results of dynamic properties obtained by simulation and experiment. The obtained results indicate high convergence. During the tests of the dynamic properties of the tested object for all the obtained modes of free vibrations of the boring bar, the relative error of the frequency value did not exceed 8%. During the tests of the static properties for all tested values of the boring bar loads, the relative error of the displacement value of the boring bar head did not exceed 3%. Such a high convergence of the results proves that the structure

Table 4. Results of measurements of the displacement of the boring bar and table frame under the influence of static loads

Sensor above the boring bar head									
Measurement	Load 98.6 N			Load 195.0 N			Load 293.8 N		
	Before	In process	Difference	Before	In process	Difference	Before	In process	Difference
1	0 µm	-236 µm	236 µm	-7 µm	-445 µm	438 µm	0 µm	-691 µm	691 µm
2	-1 µm	-218 µm	217 µm	2 µm	-443 µm	445 µm	3 µm	-679 µm	682 µm
3	0 µm	-217 µm	217 µm	3 µm	-445 µm	448 µm	4 µm	-682 µm	686 µm
Sensor under the frame									
Measurement	Load 98.6 N			Load 195.0 N			Load 293.8 N		
	Before	In process	Difference	Before	In process	Difference	Before	In process	Difference
1	505 µm	590 µm	85 µm	583 µm	750 µm	167 µm	576 µm	841 µm	265 µm
2	501 µm	585 µm	84 µm	580 µm	749 µm	169 µm	579 µm	839 µm	260 µm
3	506 µm	585 µm	79 µm	581 µm	750 µm	169 µm	579 µm	842 µm	263 µm
Mean value of the differences in the sensor's readings above the head and under the frame			**141 µm**	**Mean value of the differences in the sensor's readings above the head and under the frame**		**275 µm**	**Mean value of the differences in the sensor's readings above the head and under the frame**		**423 µm**

Table 5. Comparison of the results of numerical and experimental analyzes

Load	98.6 N	195.0 N	293.8 N
Displacement – numerical analysis	138 μm	273 μm	411 μm
Displacement – experimental research	141 μm	275 μm	423 μm

of the real object was correctly represented in the numerical model and the properties of the materials used in the theoretical analysis were very precisely defined. The results also confirmed the correctly adopted method of dividing the 3D model into finite elements during meshing, as well as the method of receiving the degrees of freedom. Thanks to the experimental verification of the simulation model, it can be said that the obtained simulation results are reliable. Simulations of the dynamic and static behavior of an object under different loading conditions can be successfully based on a digitally validated prototype and can be performed without further extensive experimental research.

It should also be mentioned that the mounting method also affects the dynamic and static properties of the boring bar [1]. In order to determine the dynamic and static properties of the boring bar during the machining process, additional tests should be carried out on the method of mounting the tool, e.g. in the tool holder of the machine tool.

The conducted tests are preliminary tests, the purpose of which is to design and manufacture a prototype of a deep hole boring bar tool with increased dynamic properties. To do this, it was necessary to verify the model of the real boring bar.

References

1. Akesson H, Smirnova T, Hakansson L. Analysis of dynamic properties of boring bars concerning different clamping conditions. Mechanical Systems and Signal Processing 2009; 23 (8): 2629-2647; 10.1016/j.ymssp.2009.05.012.
2. Al-Regib E, Ni J, Lee S-H. Programming spindle speed variation for machine tool chatter suppression. International Journal of Machine Tools and Manufacture 2003; 43 (12): 1229-1240: https://doi.org/10.1016/S0890-6955(03)00126-3.
3. Bechcinski G, Ewad H, Tsiakoumis V, Pawlowski W, Kepczak N, McMillan A, Batako DL A. A Model and Application of Vibratory Surface Grinding, Journal of Manufacturing Science and Engineering 2018; 140 (10):101011-101011-9; https://doi.org/10.1115/1.4040725.
4. Bień J, Krzyżanowski J, Poprawski W, Skoczyński W, Szymkowiak J. Experimental study of bridge structure dynamic characteristics using periodic excitation. Proceedings of ISMA 2002; 2: 555-562.
5. Brecher Ch, Baumler S, Guralnik A. Experimental Modal Analysis Using a Tracking Interferometer. CIRP Annals 2014; 63 (1): 345-348; https://doi.org/10.1016/j.cirp.2014.03.131.
6. Chen W H, Lu Z R, Lin W, Chen S H, Ni Y Q, Xia Y, Liao W Y. Theoretical and experimental modal analysis of the Guangzhou New TV Tower. Engineering Structures 2011; 33 (12): 3628-3646; https://doi.org/10.1016/j.engstruct.2011.07.028.
7. Chomette B, Carrou J-L. Operational Modal Analysis Applied to the Concert Harp. Mechanical Systems and Signal Processing 2015; 56-57: 81-91; https://doi.org/10.1016/j.ymssp.2014.10.011.
8. Ebrahimi R, Esfahanian M, Ziaei-Rad S. Vibration Modeling and Modification of Cutting Platform in a Harvest Combine by Means of Operational Modal Analysis (OMA). Measurement 2013; 46 (10): 3959-3967; https://doi.org/10.1016/j.measurement.2013.07.037.
9. Falkowicz K, Ferdynus M, Dębski H. Numerical analysis of compressed plates with a cut-out operating in the geometrically nonlinear range. Eksploatacja i Niezawodnosc – Maintenance and Reliability 2015; 17 (2): 222–227; http://dx.doi.org/10.17531/ein.2015.2.8.
10. Gagnol V, Le T P, Ray P. Modal Identification of Spindle-tool Unit in High-speed Machining. Mechanical Systems and Signal Processing 2011; 25 (7): 238-2398; https://doi.org/10.1016/j.ymssp.2011.02.019.
11. Gurraj S, Guravtar Singh M, Swastik P. Improving the Surface roughness and Flank wear of the boring process using particle damped boring bars. Materials Today: Proceedings 2018; 5 (14): 28186-28194; https://doi.org/10.1016/j.matpr.2018.10.062.
12. Karwat B, Rubacha P, Stańczyk E. Simulational and experimental determination of the exploitation parameters of a screw conveyor. Eksploatacja i Niezawodnosc – Maintenance and Reliability 2020; 22 (4): 741–747, http://dx.doi.org/10.17531/ein.2020.4.18.
13. Kilikevičius A, Rimša V, Rucki M. Investigation of influence of aircraft propeller modal parameters on small airplane performance. Eksploatacja i Niezawodnosc – Maintenance and Reliability 2020; 22 (1): 1–5, http://dx.doi.org/10.17531/ein.2020.1.1.
14. Kim N H, Won D, Ziegert J C. Numerical analysis and parameter study of a mechanical damper for use in long slender endmills. International Journal of Machine Tools and Manufacture 2006; 46 (5): 500-507; https://doi.org/10.1016/j.ijmachtools.2005.07.004.
15. Li B, Cai H, Mao X, Huang J, Luo B. Estimation of CNC Machine-tool Dynamic Parameters Based on Random Cutting Excitation Through Operational Modal Analysis. International Journal of Machine Tools & Manufacture 2013; 71: 26-40; https://doi.org/10.1016/j.ijmachtools.2013.04.001
16. Matsuo M, Yasui T, Inamura T, Matsumura M. High-speed Test of Thermal Effects for a Machine-tool Structure Based on Modal Analysis. Precision Engineering 1986; 8 (2): 72-78; https://doi.org/10.1016/0141-6359(86)90089-9.
17. Nangolo N F, Soukup J, Rychlikova L, Skocilas J. A Combined Numerical and Modal Analysis on Vertical Vibration Response of Railway Vehicle. Procedia Engineering 2014; 96: 310-319; https://doi.org/10.1016/j.proeng.2014.12.136.
18. Ondra V, Titurus B. Theoretical and experimental modal analysis of a beam-tendon system. Mechanical Systems and Signal Processing 2019; 132: 55-71; https://doi.org/10.1016/j.ymssp.2019.06.016.
19. Palanisamy P, Rajendran I, Shanmugasundaram S. Optimization of machining parameters using genetic algorithm and experimental validation for end-milling operations. The International Journal of Advanced Manufacturing Technology 2007; 32 (7-8): 644-655; 10.1007/s00170-005-0384-3.
20. Pawłowski W. Dynamic Model of Oscillation-Assisted Cylindrical Plunge Grinding With Chatter, Journal of Manufacturing Science and Engineering 2013; 135 (5): 051010-051010-6; https://doi.org/10.1115/1.4024819.
21. Pawlowski W, Kaczmarek L, Louda P. Theoretical and experimental modal analysis of the cylinder unit filled with PUR foam. Eksploatacja i Niezawodnosc – Maintenance and Reliability 2016; 18 (3): 428–435; http://dx.doi.org/10.17531/ein.2016.3.15.
22. Product data, 2006. DeltaTron® Accelerometers, Types 4514, 4514-001, 4514-002, 4514-004, 4514-B, 4514-B-001, 4514-B-002 and 4514-B-004, Brüel&Kjær.
23. Product data, 2005. Impact Hammers - Types 8206, 8206-001, 8206-002 and 8206-003, Brüel&Kjær.

24. Rahmatalla S, Hudson K, Liu Y, Eun H Ch. Finite Element Modal Analysis and Vibration-waveforms in Health Inspection of Old Bridges. Finite Elements in Analysis and Design 2014; 78: 40-46; https://doi.org/10.1016/j.finel.2013.09.006.
25. Schmitz T L, Smith K S. Machining Dynamics. Frequency Response to Improved Productivity. Boston, MA: Springer US; 2009; 8-13.
26. Sorby K, Ostling D. Precision turning with instrumented vibration-damped boring bars. Procedia CIRP 2018: 77: 666-669; https://doi.org/10.1016/j.procir.2018.08.181.
27. http://www.stressebook.com/rigid-body-mode/ Access: 10.04.2020.
28. Thomas M D, Knight W A, Sadek M M. The Impact Damper Boring Bar and Its Performance When Cutting. In: S. A. Tobias et al., editors. Proceedings of the Thirteenth International Machine Tool Design and Research Conference; 1973; 47-48; https://doi.org/10.1007/978-1-349-01857-4_7.
29. Thorenz B, Friedrich M, Westermann H-H, Dopper F. Evaluation of the influence of different inner cores on the dynamic behavior of boring bars. Procedia CIRP 2019; 81: 1171-1176; https://doi.org/10.1016/j.procir.2019.03.287.
30. Vivo A, Brutti C, Leofanti J. Modal Shape Identification of Large Structure Exposed to Wind Excitation by Operational Modal Analysis Technique. Mechanical Systems and Signal Processing 2013; 39 (1-2): 195-206; https://doi.org/10.1016/j.ymssp.2013.03.025.
31. Wang M, Zan T, Yang Y, Fei R. Design and implementation of nonlinear TMD for chatter suppression: An application in turning processes. International Journal of Machine Tools and Manufacture 2010; 50 (5): 474-479; https://doi.org/10.1016/j.ijmachtools.2010.01.004.
32. Weck M, Brecher C. Werkzeugmaschinen 5. Messtechnische Untersuchung und Beurteilung, dynamische Stabilität. 7th ed. Berlin, Heidelberg, New York: Springer; 2006; 201: 356-366.
33. Zaghbani I, Songmene V. Estimation of Machine-tool Dynamic Parameters During Machining Operation Through Operational Modal Analysis. International Journal of Machine Tools & Manufacture 2009; 49 (12-13): 947-957; https://doi.org/10.1016/j.ijmachtools.2009.06.010.
34. Zhang G P, Huang Y M, Shi W H, Fu W P. Predicting Dynamic Behaviours of a Whole Machine Tool Structure Based on Computer-aided Engineering. International Journal of Machine Tools & Manufacture 2003; 43 (7): 699-706; https://doi.org/10.1016/S0890-6955-(03)00026-9.
35. Żywica G, Kaczmarczyk T Z. Experimental evaluation of the dynamic properties of an energy microturbine with defects in the rotating system. Eksploatacja i Niezawodnosc – Maintenance and Reliability 2019; 21 (4): 670–678, http://dx.doi.org/10.17531/ein.2019.4.17.